Design of a Toolbox of RNA Thermometers — **Source link** ↗

Shaunak Sen, Divyansh Apurva, Rohit Satija, Rohit Satija ...+2 more authors

Institutions: Indian Institute of Technology Delhi, University of Texas at Austin, California Institute of Technology

Topics: Thermometer

Related papers:

- Bacterial RNA thermometers: molecular zippers and switches

- Design of simple synthetic RNA thermometers for temperature-controlled gene expression in Escherichia coli

- Rapid cell-free forward engineering of novel genetic ring oscillators

- Tunable thermal bioswitches for in vivo control of microbial therapeutics.

- De novo design of heat-repressible RNA thermosensors in E. coli

Article

Design of a Toolbox of RNA Thermometers

Shaunak Sen, Divyansh Apurva, Rohit Satija, Dan Siegal, and Richard M. Murray

Just Accepted

Design of a Toolbox of RNA Thermometers

Shaunak Sen,*,† Divyansh Apurva,‡ Rohit Satija,‡,§ Dan Siegal,¶,∥ and Richard M.

Murray¶

†*Department of Electrical Engineering, Indian Institute of Technology Delhi, Hauz Khas,*

New Delhi 110016, INDIA

‡*Department of Biochemical Engineering and Biotechnology, Indian Institute of Technology*

Delhi, Hauz Khas, New Delhi 110016, INDIA

¶*Division of Biology and Biological Engineering, California Institute of Technology,*

Pasadena, CA 91125, USA

§*Institute for Cellular and Molecular Biology, University of Texas at Austin, Austin, TX*

78712, USA

∥*Schafer Corporation, Arlington VA 22203, USA*

E-mail: shaunak.sen@ee.iitd.ac.in

Abstract

Biomolecular temperature sensors can be used for efficient control of large-volume bioreactors, for spatiotemporal imaging and control of gene expression, and to engineer robustness to temperature in biomolecular circuit design. While RNA-based sensors, called 'thermometers', have been investigated in both natural and synthetic contexts, an important challenge is to design diverse responses to temperature, differing in sensitivities and thresholds. We address this issue by constructing a library of RNA thermometers, based on thermodynamic computations, and experimentally measuring their activities in cell-free biomolecular 'breadboards'. Using free energies of the minimum free energy structures as well as melt profile computations, we estimated that

a diverse set of temperature responses were possible. We experimentally found a wide range of responses to temperature in the temperature range 29 °C–37 °C, with fold-changes varying over 3-fold around the starting thermometer. The sensitivities of these responses ranged over 10-fold around the starting thermometer. We correlated these measurements with computational expectations, finding that while there was no strong correlation for the individual thermometers, overall trends of diversity, fold-changes, and sensitivities were similar. These results present a toolbox of RNA-based circuit elements with diverse temperature responses.

Keywords

RNA thermometers, synthetic biology, cell-free breadboard, computational design, free energies, melt profiles, temperature sensor

1 Introduction

Biomolecular temperature sensors, which convert temperature into a biologically functional response, can have multiple applications. These include, for example, large-volume bioreactors, where such sensors allow the use of heat as an inducer, which may be more convenient than a chemical-based inducer. As another example, these sensors can be used to spatiotemporally control pathways inside cells and tissues through local heating induced by electromagnetic waves in the millimetre range (*1*, *2*). In the case that these regulate the expression of reporters, they can be used for spatiotemporally precise imaging as well. Furthermore, temperature sensors may find application in engineering temperature compensation in biomolecular circuit design, where it is often desired to have specifically-tailored responses to temperature to counteract, and hence cancel, other changes with temperature (*3*, *4*). Finally, in addition to cell-based applications, there are also potential applications for temperature sensors in cell-free settings, including temperature detection in paper-based assays (*5*) or

temperature compensation for cell-free circuits (*6–8*). To meet these needs, it is desirable to have a toolbox of temperature sensors with different sensitivities and thresholds.

Temperature-sensing RNA molecules, called 'RNA thermometers', operate in diverse natural contexts, mediating cellular behaviours such as heat-shock response and pathogenesis (*9*). There are many mechanisms for the operation of an RNA thermometer, each of which depend on a temperature-dependent conformational change. At its simplest, an RNA thermometer consists of an RNA sequence containing the ribosome binding site (RBS, Fig. 1A). At a permissive temperature, the ribosome can access this RBS and translation proceeds efficiently. At a restrictive temperature, the RNA sequence folds in such a manner so as to prevent this access and inhibit translation. Examples include the *rpoH* gene mediating heat-shock response in *E. coli* (*10*), the *agsA* gene regulating the heat-shock response in *S. enterica* (*11*), the *hsp17* gene regulating heat-shock response and photosynthesis in *Synechocystis* sp. PCC 6803 (*12*), and the *cIII* gene regulating the life cycle of phage λ (*13*). While these natural examples can have a relatively complicated secondary structure with multiple stems, hairpin loops, and bulges, RNA thermometers have been designed with simpler secondary structures, with only a single stem-loop protecting the RBS (*14*). The temperature response of these thermometers was designed on the basis of the melting temperature of the minimum free energy structure, with an increased stem length, a smaller hairpin loop, or a reduction in the number of bulges resulting in an increase in the melting temperature (*14–16*). More recently, RNA thermometers have also been designed to be heat-repressible using an RNase E-mediated mechanism (*17*). These previous studies have provided important results towards an elucidation of mechanisms underlying RNA thermometer operation, modulation of their response to temperature, and towards prediction of their behaviour.

There are at least three striking aspects about the functioning of RNA thermometers. The first aspect is the startling complexity that can exist in the secondary structure of the naturally occurring RNA thermometers in comparison to the synthetic ones. The second

A

OFF

Loop

Bulge

Stem

$+\Delta T$

$-\Delta T$

ON

RNA

■ ribosome binding site (RBS)

B RNA Thermometer Activity

M

$\dfrac{m + M}{2}$
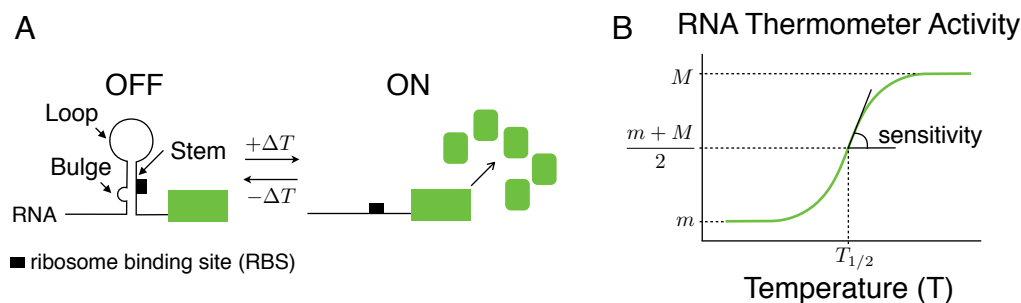
sensitivity

m

$T_{1/2}$

Temperature (T)

Figure 1: Temperature response of a RNA thermometer. A. Illustration of the functioning of a simple RNA thermometer. Structural features such as loops, bulges, and stems are indicated. B. The green solid line represents the activity of the RNA thermometer as a function of temperature. Key quantitative feature of the response such as threshold and sensitivity are emphasized.

aspect is the large number of different secondary structures possible, in addition to the minimum free energy structure, that an RNA thermometer can adopt at any given temperature. The activity of a thermometer can be directly dependent on the proportion of these different structures and their respective activities. The third aspect is how even a one base change in sequence can qualitatively change the temperature response. In particular, among the published synthetic thermometers (*14*), a one base change can shift the response from linear-like to switch-like (U2 and U9 in (*14*)). Similar instances have also been noted in natural contexts such as in the *agsA* gene of *S. enterica* (*11*) and in the *hsp17* gene of *Synechocystis* sp. PCC 6803 (*12*). The role of these factors in determining the sensitivity of an RNA thermometer is generally unclear.

Here, our objective is to design a set of RNA thermometers with different sensitivities in their response to temperature (Fig. 1B). We used a combination of experimental measurements in cell-free biomolecular 'breadboards' and computations of RNA secondary structures to achieve this objective. We studied a set of existing synthetic thermometers, finding consistency with existing results and among our experimental and computational analyses. Next, we constructed a library of thermometers by systematically changing a thermometer sequence one base at a time, finding, computationally, that a range of temperature responses with different sensitivities is possible. Finally, we constructed this library and found a variety of

responses in the temperature range 29 °C–37 °C, with over 10-fold difference in sensitivities and over 3-fold difference in fold-changes around the starting thermometer. When assessed against the computational expectations, we find that the overall systems-level trends of diverse sensitivities and fold-changes match reasonably well. These results provide a toolbox of temperature-regulatory biomolecular circuit components for synthetic biology applications.

2   Results and Discussion

2.1   Analysis of Existing RNA Thermometers

We started our investigation with an analysis of two existing synthetic RNA thermometers X and Y (respectively, U2 and U9 from (14)). These differ in sequence by only one base, yet have qualitatively different responses to temperature (Fig. 2A).

To get an initial estimate of thermometer activity as a function of temperature, plasmids (14) containing either of these thermometers in the 5'-UTR region of a gene coding for a green fluorescent protein (GFP-trps16) were spotted onto LB-agar plates and imaged in a fluorescence imager (Fig. 2B). We found that the fluorescence of both constructs was larger at 37 °C than at 29 °C, consistent with previous results. Further, there were differences between X and Y in terms of the extent of increase, with cells containing the X construct being more fluorescent than the cells containing the Y construct at 37 °C, also consistent with previous results.

For a more quantitative estimate, we used an *E. coli* cell-extract-based biomolecular breadboard, which allows transcription and translation in a rapid prototyping platform (18). Plasmid DNA was incubated in the breadboard at different temperatures — 29 °C and 37 °C — and the GFP expression was measured at $t = 150$ minutes. We found that the thermometer activity of X increased with temperature (Fig. 2C). While the mean value of the thermometer activity of Y also increased with temperature, the error bars overlapped. Therefore, the activity of thermometer X increased more than that of Y. These results

A

RBS

X: GGAUCCCUCA CUUACUAGUC UGCAGAAGGA GAUAUACCCA UGG

Y: GGAUCCCUC CUUACUAGUC UGCAGAAGGA GAUAUACCCA UGG

B

Cells, each disc is a spot

29 ℃ 37 ℃   29 ℃ 37 ℃

X   Y

GFP   GFP

C

Cell-free breadboard

D

X   Y

-5.15 kcal/mol   -8.95 kcal/mol
(minimum free energy
structure, 29 ℃)

E
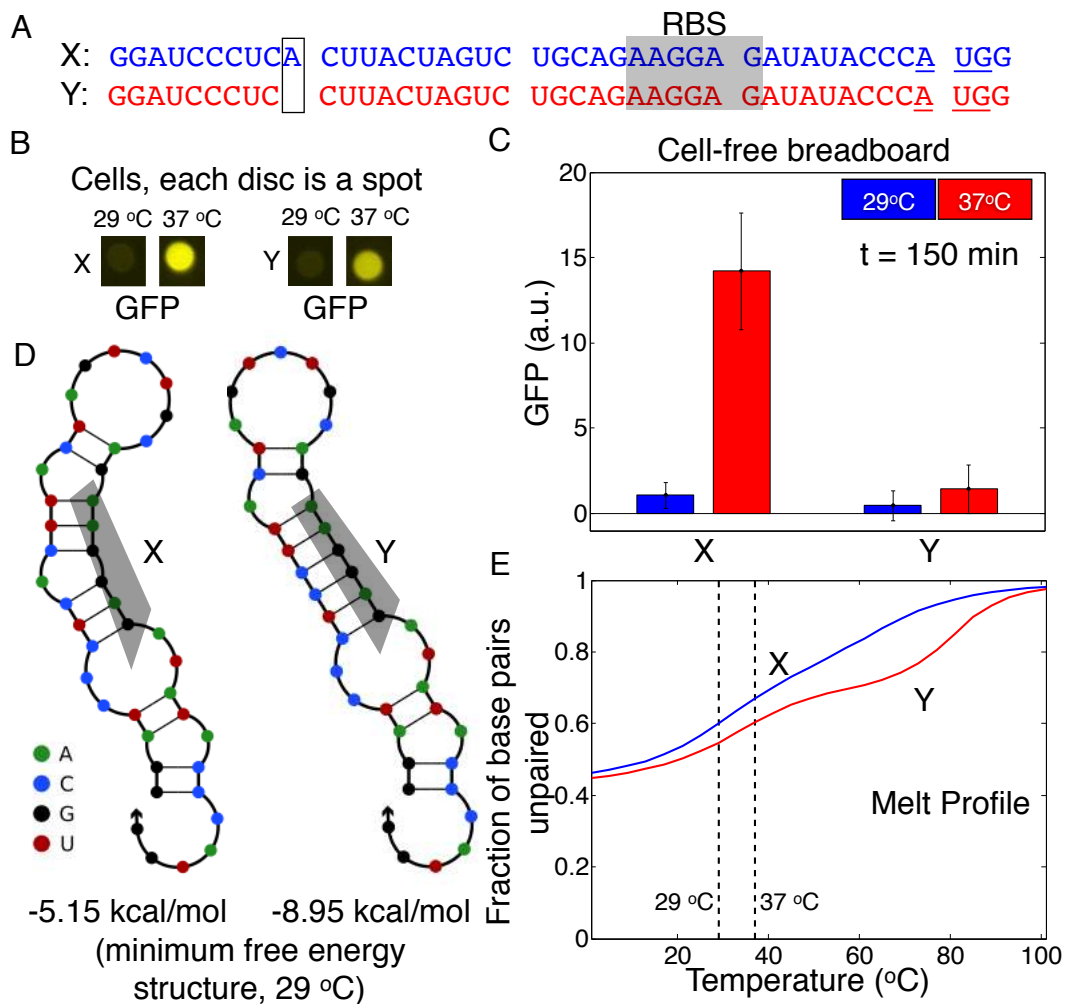
Figure 2: Characterisation of two existing thermometers computationally and experimentally. A. Thermometer sequences. B. Thermometer activity in cell spots. Intensity represents green fluorescence (in arbitrary units). C. Quantification of thermometer activity in cell-free breadboards. Each bar is a mean of three separate measurements with the error bars representing one standard deviation. D. Secondary structures of the minimum free energy structure and corresponding free energies. The grey box shades the RBS. E. Computationally obtained melt profiles of the thermometers.

are consistent with expectations based on published results as well as with the cellular fluorescence estimates presented above.

In addition to the effect of temperature on the secondary structure of the RNA thermometers, it is likely that temperature affects other aspects of the measurement assays described above. These include the fluorescence parameters of GFP, the activity of RNA polymerase during transcription, and the growth rate of cells. However, these factors should affect both thermometers in a similar fashion. Therefore, in our investigations, we focus on the relative difference in thermometer activities.

To assess the similarity between the experimental measurements and theoretical expectations, we analyzed the thermometer sequences using NUPACK, an algorithm that can compute nucleic acid thermodynamics (19). Given an RNA sequence, NUPACK can compute the minimum free energy and the corresponding structure at different temperatures. We computed these structures at 29 °C using the sequences of X and Y and found that they were largely similar (Fig. 2D). The major difference is the presence of a bulge in the stem containing the RBS in X. Further, the free energy of the X structure is larger than that of Y. These suggest that the thermometer X should be less stable than Y, and consequently that expression of GFP controlled by X should be higher than that of GFP controlled by Y at each temperature. This is consistent with results established previously and with the experimental measurements presented above.

For a given temperature, in general, there are multiple structures that an RNA molecule can adopt. These other structures may also contribute to the activity of an RNA thermometer. To take these into account, we used NUPACK to calculate the fraction of unpaired bases as a function of temperature. As the thermometer activity is proportional to the extent of its melting, we used this fraction as another measure of its activity. Comparisons of the melt profiles of X and Y show that X melts more than Y at each temperature (Fig. 2E). These are also consistent with our expectations.

Together, these results, analysing existing RNA thermometers both experimentally and

computationally, are consistent with published results and with each other.

2.2 Computational Analysis of a Thermometer Library Suggests a Diversity of Responses

Noting that the two thermometers studied above, with different responses, differed in sequence by only one base, we wondered whether other one base changes to the thermometer sequence could generate the desired diverse set of temperature responses. There are 43 bases in the thermometer X, with a deletion at the 10th position giving the thermometer Y (Fig. 3A). Other one base changes include a deletion at any other location as well as replacing the existing nucleotide with the other three possibilities, for a total of $4 \times 43 = 172$ possibilities. For reasons of scale, we focussed on the 10th position as well as the positions involved in the secondary structure base pairing of the minimum free energy structure. This gives rise to a $4 \times 19 = 76$ variants (Fig. 3A, listed in Supplementary Information A).

To check if these different thermometers could indeed generate a diversity in responses, we used NUPACK to compute their free energies and melt profiles. The free energies computed at 29 °C show a diversity of values, across the range from those of X and Y (Fig. 3B). This suggests that different responses may be possible in this library. Similarly, the melt profile computations show that a variety of responses could be generated (Fig. 3C). These include those melt curves that are more linear-like compared to that of X as well as more switch-like. Considering the derivative of the melt curves emphasises the diversity in slopes that may be obtained (Fig. 3C, inset). These computations suggest that the construction of such a library may achieve the objective of different sensitivities in the temperature response.

2.3 Experimental Characterization of a Thermometer Library

We experimentally constructed a thermometer library using standard procedures described in the Methods section. On screening, we recovered 38 out of the 76 potential members of

A

Library size = 19 x 4 = 76

X: GGAUCCCUCA CUUACUAGUC UGCAGAAGGA GAUAUACCCA UGG

RBS

AACA	AAAC	AAA	AA		CA		CA	AA
CCGC	GCGG	GCC	GC		GC		GC	GG
UUUG	UGUU	UGG	UG		UU		UG	UU

B

C Melt Profile

Figure 3: Computational analysis of a thermometer library. A. Thermometer sequences considered in the library. The starting sequence, of thermometer X, is given in blue . Arrows indicate the base changes considered for the library, with a dash symbol denoting deletion. The red dash indicates the deletion that gives thermometer Y. B. Histogram representing the free energy of the minimum free energy structure at 29 °C. The locations of the thermometers X and Y are highlighted using blue and red arrows, respectively. C. Melt profiles of thermometer library. The blue line represent the melt profile of thermometer X. The light grey lines represents the melt profiles of the remaining thermometers. The red steep and green shallow lines are highlighted thermometers whose melt profiles show, relative to thermometer X, a lower and higher sensitivity, respectively. Inset shows the derivatives of the melt profiles computed through a first difference approximation.

the library. We measured the activities of these thermometers in molecular breadboards at three different temperatures — 29 °C, 33 °C, and 37 °C (Fig. 4A, B). We find a variety of responses that are different from the starting response. This is so even though the various responses arise from a thermometer sequence that differs from the starting thermometer sequence by only one base. All the responses increase with increasing temperature, however the extent of increase relative to temperature is different.

Temperature dependence of global factors such as the fluorescence parameters of GFP or the activity of RNA polymerase may contribute to the individual thermometer measurements. They should, however, affect all thermometers in a similar fashion. Therefore, we focus on relative difference in the thermometer activities. Further, we measured the temperature response of a +C construct, which was used as a positive control for the functioning of the breadboard reactions (*18*). The +C construct has GFP under the control of a constitutive promoter (please see Materials and Methods Section 3.3 for details). The activity of +C increased with temperature, possibly due to a combination of the global factors and its inherent temperature dependence (Supplementary Information B). While the overall values at each temperature are higher than that of the parent thermometer X, the fold-change is smaller than that of X (Fig. 4C). Therefore, the temperature response of +C and X are different, suggesting that these temperature responses are not solely due to the temperature dependence of global factors.

To quantify different features of this library, we computed the maximum fold-change and the sensitivities of the response in the given temperature range (Fig. 4C, D). We find that the maximum fold-change ranges from 3.5-fold to above 10-fold (Fig. 4C). These fold-changes vary over a 3-fold range around the starting thermometer and were higher than that of the +C construct. Further, the basal activity at 29 °C changes by over 10-fold. We noted a slight downward trend in the maximum fold-change as the basal activity increases. Finally, we find that the responses have diverse sensitivities, estimated from the slope of the response from 29 °C to 33 °C and from 33 °C to 37 °C, varying by over 10-fold range around the starting

thermometer (Fig. 4D). These results show that there is a diverse set of thermometer profiles in this library.

To check if similar diversity is observable inside cells, we spotted cells containing these thermometer constructs at different temperatures and imaged their fluorescence (Supplementary Information C). We found that, in general, the fluorescence values increased with temperature. There were differences in the rate of increase which points to a diversity in thermometer responses. In particular, consideration of fluorescence images at 33 °C highlights this diversity. This suggests that the thermometer library can give diverse responses inside cells.

2.4   Assessment of Match between Computations and Experiments

We assessed the match between these experimental measurements and our expectations based on the computation of free energies and melt profiles.

We compared the free energy of the minimum free energy structure with the experimentally measured expression level for each thermometer and at the different temperatures (Fig. 5A). If the correlation were perfect, we would expect a linear trend. This is not seen.

The correlation between the measurements and free energies of individual thermometers is weak $(r = -0.43, p < 10^{-4})$. The $\{r, p\}$ values for the correlations considered separately for the temperatures 29 °C, 33 °C, and 37 °C, are $\{-0.11, 0.52\}$, $\{-0.10, 0.55\}$, and $\{-0.13, 0.43\}$, respectively. At best, the cluster of points appear to be below a straight line, in a triangular-shaped region. Next, we checked whether the overall trends of fold-change and diverse sensitivities were observed in the library. To obtain the computational version of the fold-change plot, we computed the difference in the free energies of each thermometer and plotted it against the free energy at the lowest temperature (Fig. 5B). The overall trend of the fold-change plot (Fig. 5B) is of a decreasing nature, similar to that obtained experimentally (Fig. 4C). Similarly, the slope plot corresponding to the free energies, where the difference in free energies at the successive temperatures are plotted against each other (Fig.
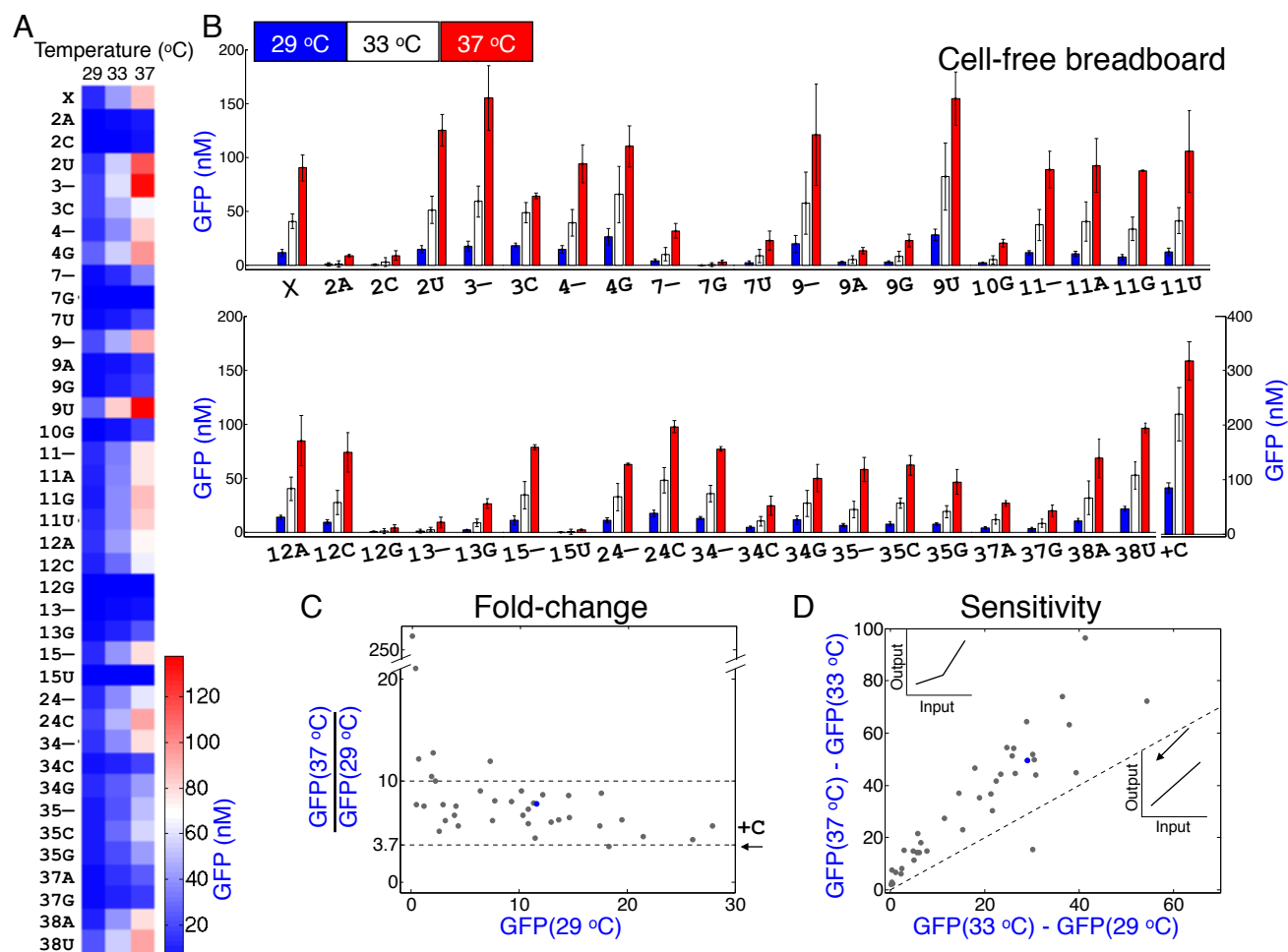
Figure 4: Experimental measurements of the thermometer library show a variety of responses. A. Rows represent activity levels of different thermometers. The activity levels are the mean of three separate measurements. These values are normalised using a GFP calibration performed at 29 °C. B. Replotting of data from A. Each set of three bars represents the activity level of a different thermometer. +C is the construct used as positive control for the functioning of the breadboard reactions. The bar colors blue, white, and red represent the temperatures 29 °C, 33 °C, and 37 °C, respectively. The height of the bars corresponds the mean levels of three separate measurements with the standard deviation shown as the error bar. Four separate measurements were taken for +C. C & D. Each grey dot represents an individual thermometer. A blue dot is used for the starting thermometer X. In C, the thermometer 7G is omitted as the fold-changes, due to negative background-subtracted value at 29 °C, is negative. The lower black dashed line represents the fold-change value of +C. The black dashed line in D is such that the x- and y-coordinates of points on it are equal. As such, it represents ideal linear responses. Inset graphs in D are illustrative input-output responses. The inset graph indicated to be on the dashed line represents an ideal linear response. The inset graph at the upper left corner represents a steeper input-output response.

5C, individual sensitivities are correlated in Supplementary Information D), shows that diverse sensitivities are possible, a trend that is similar to that seen experimentally (Fig. 4D). Therefore, the overall trends of fold-change and sensitivity are similar, but there is at best weak correlation between the measurements and free energies of individual thermometers.

A possible reason underlying the discrepancies observed could be that the free energy considered is that of the minimum free energy structure, which may only be a small fraction of the overall ensemble of structures. To investigate this, we shaded the dots in Fig. 5A according to the fraction of the minimum free energy structure in the ensemble of structures. We find that most of the dots are shaded in lighter versions of grey, indicating that the minimum free energy structure may be only a small fraction of the overall ensemble. This could underlie the weak correlation observed. To investigate this further, we considered the free energy of the entire ensemble and assessed this against the experimental measurements. We find similar trends (Fig. 5D-F):

The individual thermometer responses do not show a strong correlation, although these look better (Fig. 5D, $r = -0.54$, $p < 10^{-4}$) than the one using the free energy of the minimum free energy structure (Fig. 5A, $r = -0.43$, $p < 10^{-4}$). The $\{r, p\}$ values for the correlations considered separately for the temperatures 29 °C, 33 °C, and 37 °C, are $\{-0.16, 0.34\}$, $\{-0.17, 0.29\}$, and $\{-0.22, 0.19\}$, respectively. Further, the overall trends match reasonably well.

To assess the match further, we compared the experimental measurements with the melt profile, the fraction of bases unpaired at each temperature (denoted $P_{melt}(T)$, Fig. 6A). The plot does not show a strong correlation ($r = 0.44$, $p < 10^{-4}$). The $\{r, p\}$ values for the correlations considered separately for the temperatures 29 °C, 33 °C, and 37 °C, are $\{0.12, 0.48\}$, $\{0.09, 0.61\}$, and $\{0.09, 0.61\}$, respectively. On the other hand, when the fold-change and sensitivity of the response is assessed from the melt profiles, the trends are similar to those observed experimentally (Fig. 6B-C, individual sensitivities are correlated in Supplementary Information D). The above plots were based on the melt profile of the entire
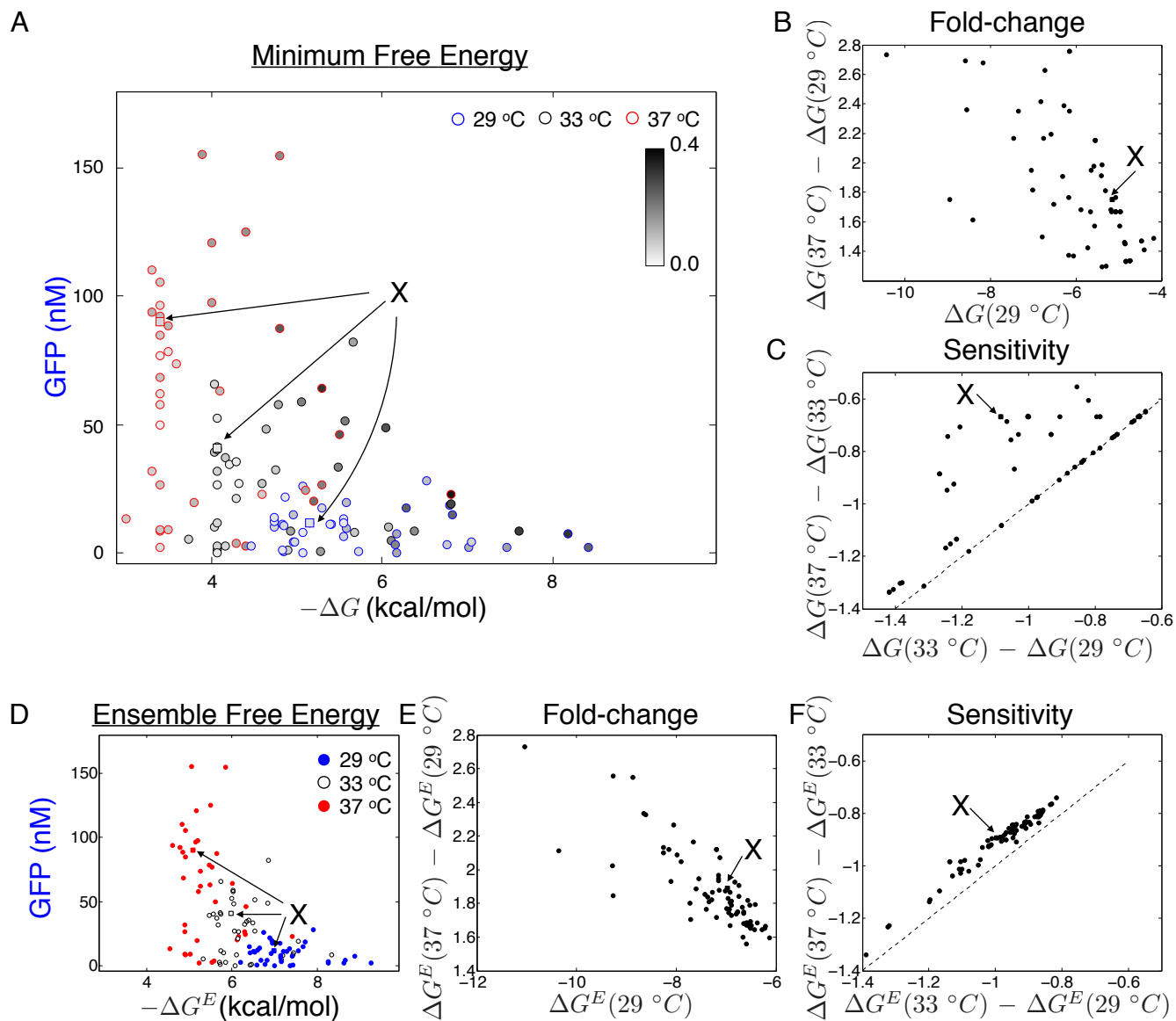
Figure 5: Assessment of experimental measurements and computations. A. Each dot represents an individual thermometer plotted with its experimentally measured value on the Y-axis and the free energy of the minimum free energy structure on the X-axis. The blue, black, and red circles represent the temperatures 29 °C, 33 °C, and 37 °C, respectively. Each circle is shaded according to the equilibrium probability of the minimum free energy structure. The starting thermometer is highlighted as a square marker and additionally indicated with an arrow. B. Each dot represents an individual thermometer plotted with its net difference in free energy of the minimum free energy structure between the temperatures 29 °C and 37 °C on the Y-axis and the free energy of the minimum free energy structure at 29 °C on the X-axis. C. Each dot represents an individual thermometer with its net difference in free energy of the minimum free energy structure between the temperatures 33 °C and 37 °C on the Y-axis and the net difference in free energy of the minimum free energy structure between the temperatures 29 °C and 33 °C on the X-axis. Dashed line represents where the dots would lie if the response was linear in this temperature range. D–F. Same plots as above, but considering the free energy of the ensemble rather than just that of the minimum free energy structure. As it is the entire ensemble that is considered, there is no shading of the circles in D. Instead they are filled with the colors blue, white, and red for temperatures 29 °C, 33 °C, and 37 °C, respectively.

sequence. To check if a different part of the sequence gives a better match, we considered the average equilibrium probability that the base pairs belonging to the RBS are unpaired (denoted $P_{melt}^{RBS}(T)$, rather than the entire thermometer sequence. We computed this average probability and assessed it with the experiments, both in terms of the correlation with the individual measurements (Fig. 6D) as well as for the trends within it (Fig. 6E-F). The correlations in the individual measurements are weak ($r = 0.22$, $p = 0.02$). The $\{r, p\}$ values for the correlations considered separately for the temperatures 29 °C, 33 °C, and 37 °C, are $\{0.23, 0.16\}$, $\{0.15, 0.38\}$, and $\{0.10, 0.55\}$, respectively.

Through the computational assessments considered above, we conclude that the overall trends are similar to those observed experimentally. However, we note that the individual values do not exhibit a strong correlation. Possible reasons underlying this discrepancy may be in the assumptions made in the computations, such as the choice of parameter values, the set of possible structures, and the folding kinetics, which may not hold in experimental conditions.

2.5　Summary and future work

Temperature-sensing RNA thermometers can have multiple applications. Using a combination of experimental measurements in cell-free biomolecular breadboards and computations of RNA thermodynamic parameters such as free energies, minimum free energy structure, and melt profiles, we have developed a toolbox of RNA thermometers, supported by three primary conclusions. First, we found broad agreement with our methodologies and previous measurements on a set of thermometers. Second, we computationally found that a wide array of temperature responses are possible in a library of thermometers, each member of which is a one base change of a starting thermometer sequence. Third, we synthesized such a library and found a diversity of responses, with over 10-fold difference in sensitivities and fold-changes varying over 3-fold range around the starting thermometer. The overall trends of the responses obtained computationally and measured experimentally match reasonably
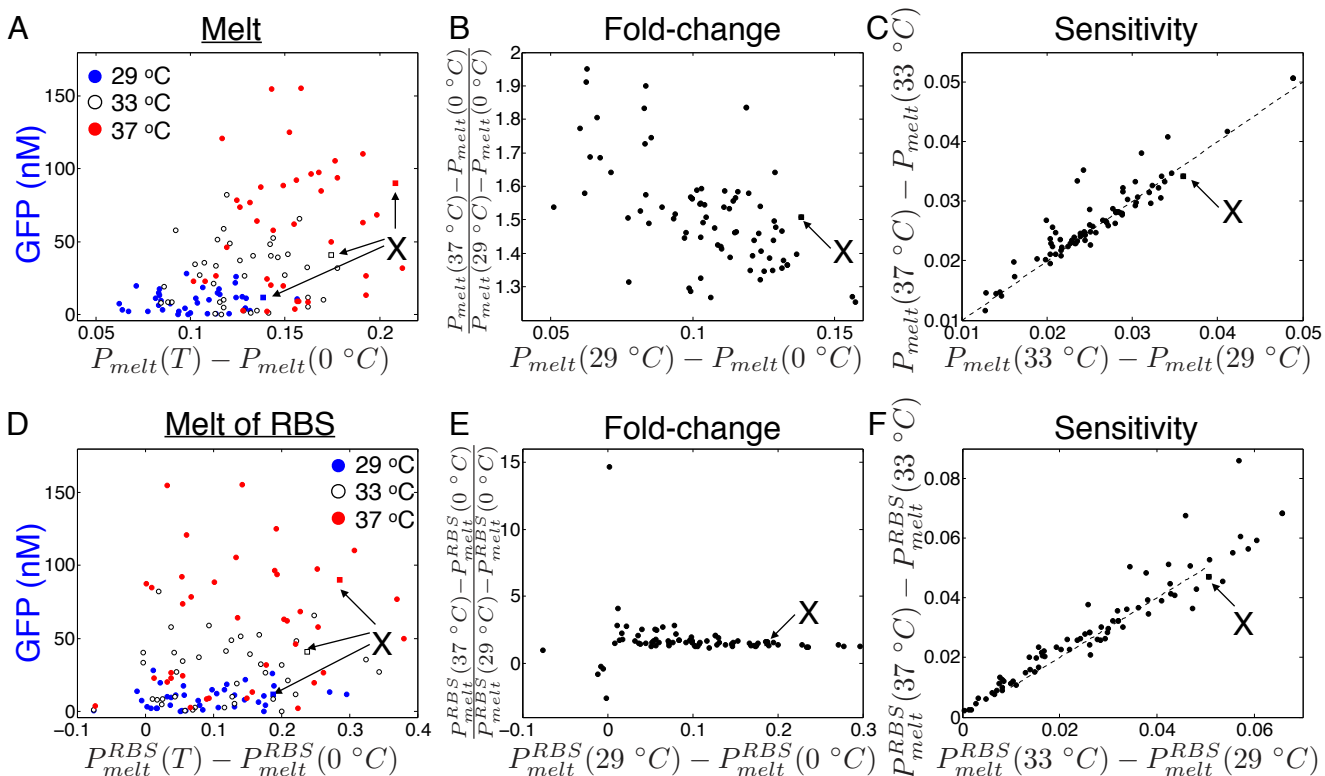
Figure 6: Assessment of experimental measurements and melt profile computations. A. Each dot represents an individual thermometer, plotted with its experimental value on the Y-axis and the extent of melt on the X-axis. The circles filled with colors blue, white, and red represent the temperatures 29 °C, 33 °C, and 37 °C, respectively. The starting thermometer is highlighted as a square marker and indicated with an arrow. B. Each dot represents an individual thermometer, plotted with its net difference in melt profile between the temperatures 29 °C and 37 °C on the Y-axis and the extent of melt at 29 °C on the X-axis. C. Each dot represents an individual thermometer, with the melt response slope based on the temperatures 33 °C and 37 °C on the Y-axis and the slope based on the temperatures 29 °C and 33 °C on the X-axis. Dashed line represents where the dots would lie if the response was linear. D–F. Same plots as above, but considering only the melt profile of the RBS region.

well, although the individual values do not show a strong correlation.

In our measurements, we focus on comparing thermometer activities relative to the parent thermometer X. A reason for this is that temperature, being a global variable, may affect many aspects of the measured system, such as the fluorescence properties of GFP and the RNA polymerase activity. The observation of diverse temperature responses in the thermometer library suggests that the measured responses are not solely due to these global factors. Further, we report the temperature response of a +C construct that is different from the parent thermometer X. The temperature response of the +C construct is a combination of these global factors as well as its own temperature dependence. The observation that this is different from the parent thermometer X also indicates that the measured responses are not solely due to the global factors.

It is interesting that even a one base change in the sequence of an RNA thermometer can generate a substantial change in the temperature response. We have observed this in our results both computationally and through the experimental measurements. It is likely that relatively complicated secondary structures that are found in the natural contexts may have evolved so that sensitivity to single base alterations is minimized.

The lack of strong correlation observed in the computations and breadboard measurements is also interesting. To understand this gap further, we looked at few individual thermometers in greater detail.

Consider the mutation 2A, whose free energies of the minimum free energy structure as well as of the ensemble are greater than or equal to that of starting thermometer X at all three temperatures 29 °C, 33 °C, and 37 °C (Supplementary Information E). Based on this, it is expected that the corresponding fluorescence values would be higher. This is not seen and the fluorescence level of thermometer 2A is less than that of the starting thermometer X at all the three temperatures 29 °C, 33 °C, and 37 °C (Fig. 4B). A possible resolution of this gap is in considering the melt profile, and specifically its derivative (Supplementary Information E). Each point on the derivative of the melt curve denotes the extent of "melting"

at that temperature. The melting of thermometer 2A is less than that of X, especially in the temperature range where measurements are taken. This indicates that X melts more in this temperature range than 2A and this "opening up" could underlie its larger fluorescence. We looked at the minimum free energy structures of these thermometers and found that structures away from the hairpin stem that encloses the RBS have opened up. This suggests that it is the melting away of these smaller structures and not the hairpin stem only, that is relevant at these temperatures. The hairpin stem may, of course, be melting to some level. Therefore, one possibility is that the thermometer melting, especially in terms of the non-hairpin stem structures, could be one feature to look at.

To explore this line of reasoning further, we looked at thermometer 2C (Supplementary Information E). This is similar to 2A in many respects. The measured fluorescence values are lower than that of X (Fig. 4B), even though the computed free energies are higher. The extent of melting, however, is lower than that of X and could underlie its measured response relative to X. The minimum free energy structures indicate that the hairpin stem is still closed around the RBS but some structure above and below it have melted away, pointing to the importance of these structures surrounding the RBS bound region.

The thermometer 2U is brighter than thermometer X, especially at 37 °C (Fig. 4B). The free energies of the minimum free energy structure and the ensemble, however, are larger than those of X. We computed the melt profile and its derivative for this thermometer to shed some light on this gap. We find that the extent of melting of 2U near the measured temperature range is comparable to, and in some parts larger than, that of X. The computed minimum free energy structures show that the structure inside the hairpin melts away. We note that, in this case, the minimum free energy structure is a larger fraction of the ensemble in comparison to X and so conclusions drawn from the minimum free energy structure to the entire ensemble may be more relevant in this case.

The measurements of thermometer 3– are also brighter in relation to X (Fig. 4B), similar to those of thermometer 2U. Further, the free energies of 3– are lower than that of X

(Supplementary Information E). As in the case of thermometer examples considered above, consideration of the extent of melting provides a way to rationalise the computations and the experiments (Supplementary Information E). In particular, the melting of the thermometer 3– near the temperature range of measurement is comparable to, and in some cases larger than, that of X. Furthermore, the smaller structures that do not enclose the RBS melt away in the minimum free energy structure, suggesting that these smaller structures may play a key role in making the RBS more accessible to the ribosome.

The measurement of thermometer 3C is similar to that of X (Fig. 4B), especially that of temperatures 29 °C and 33 °C. This is so even though the computed free energies are more stable (Supplementary Information E) based on which we would expect the measurement values to be lower. Consideration of the melt profile does not completely resolve this gap, unlike in the previous examples. The extent of melt is also low compared to X. The minimum free energy structure also does not change in the temperatures 29 °C, 33 °C, and 37 °C, where the principal binding is in the stem that encloses the RBS. It could be that the smaller structures have already melted away before the measured temperature range and the response is due to the melting of the main stem. In this case, the interpretation of the melt profile in terms of the experiments is not completely clear.

We conclude that consideration of the melt profile may be used as a guideline for the design of thermometers, in addition to those of free energies and the minimum free energy structure. In most of the thermometers discussed above, we find that it can add insight into the extent of melt to be expected from a thermometer. It further draws attention to the point that, in addition to the main hairpin stem that occludes the RBS, other smaller neighboring structures in the RNA structures may play a key role in determining the temperature response. This is especially so in the range of temperatures considered here.

An immediate task for future work is to correlate the experimental measurements in the cell-free breadboards with quantitative measurement of fluorescence in a population of cells or at the level of the single cell. Preliminary correlation performed using a quantitation of

the cell spot assays is not strong (Supplementary Information F). As a next step, it may be useful to demonstrate functional applications of these thermometers, particularly in the development of circuits that need to interface with temperature. An example of this is to use these as the input stage of a pulse generating incoherent feedforward loop circuit, thereby generating a pulse of gene expression triggered by temperature.

The design and development of new biomolecular circuits and components, often based on naturally occurring ones, can facilitate various synthetic biology applications, such as in metabolic engineering, agriculture, and medicine (*20*). RNA is an attractive substrate for this, due to its substantial regulatory and sensing potential (*21*, *22*) as well as the availability of computational tools to estimate its behaviour and help in the design process (*23*, *24*). Indeed, RNA molecules can be designed to sense extremely specific signals such as metabolites or other RNAs (*25*) as well as more global signals such as temperature (*26*). Here, we have presented experimental and computational results for the development of RNA-based temperature sensors. In addition to the multiple applications mentioned above, such as in large bioreactors, for thermal imaging and control of gene expression, for designing temperature robustness, as well as in cell-free contexts, these results highlight the usefulness of RNA for synthetic biology as well as advances required to completely understand relatively simple mechanisms.

3   Materials and Methods

3.1   Computational Analysis

All thermometer sequences were analyzed using the computational tool NUPACK (*19*). This was used to compute the minimum free energy structure and its free energy, the ensemble free energy, as well as the fraction of bases unpaired. All of these values were obtained for the desired range of temperatures.

All correlation coefficients were obtained using the function *corrcoef* in MATLAB. The

p-values test the hypothesis of no correlation.

3.2   Plasmids and Bacterial Strains

For the estimate of thermometer activity in cells, plasmids pBSU2 and pBSU9 (*14*) containing the thermometers in the 5'-UTR region of a green fluorescent protein (GFP-trps16) were transformed into *E. coli* (JM109). These cells were then spotted on LB-agar plates containing 100 μg/ml carbenicillin and incubated overnight at different temperatures. Subsequently, their fluorescence was imaged in UV light in a gel imager (AlphaImager) (Fig. 2B).

To construct the library, green fluorescent protein in pBSU2 was replaced from gfp-Trp16 to deGFP-T500, a variant previously used in the cell-free breadboard (*18*). deGFP-T500 was amplified using PCR and digested with restriction enzymes NcoI and HindIII. Similarly, pBSU2 was digested with these restriction enzymes and further treated with Antarctic Phosphatase (NEB). These were then ligated and transformed.

The desired thermometer sequences were constructed using PCR. For each thermometer, four sets of primers were used. The first primer was homologous to a sequence approximately 250 bases upstream of the promoter of the plasmid pBSU2-deGFP. The second primer was homologous to the X thermometer and contained the desired promoter. These two primers were used to amplify the promoter region with some part of the thermometer. The third primer was designed to substantially overlap with the second primer and contained the desired mutation. The fourth primer was designed to bind to a sequence approximately 250 bases downstream of the terminator of the plasmid pBSU2-deGFP. These two primers were used to amplify the green fluorescent protein and part of the thermometer region. Finally, the two PCR products were fused using the first and the fourth primer. All primers were ordered from IDT Inc. (San Diego, California, USA). All PCR reactions were carried out using Phusion® Hot Start Flex 2X Master Mix (NEB).

Finally, after amplification, these thermometers were ligated into the vector backbone of

pBSU2. For this, these PCR products were mixed, and digested with the restriction enzymes SacI and HindIII. Similarly, the vector pBSU2-deGFP was digested and additionally treated with Antarctic Phosphatase (NEB). This mixture of thermometers and the vector were ligated using the Quick Ligase Kit (NEB) and transformed into chemically competent *E. coli* JM109 cells. The obtained colonies were screened by sequencing using the M13 primers. On screening, we recovered 38 different variants from the library. Additionally, one of the screens was found to be the original thermometer. These 39 thermometers were used for measurements (Fig. 4).

3.3   Measurements in a Cell-free Biomolecular Breadboard

We used an *E. coli* cell-extract-based biomolecular breadboard that allows transcription and translation using previously described protocols (*18*). The protocol involves performing reactions in a volume of 10 μl. Each reaction consisted of cell extract, buffer, plasmid DNA (5 nM), and water. The reactions were incubated at desired temperatures and measurement was performed after 150 minutes. All breadboard measurements were performed in black transparent-bottomed 384-well plates (Perkin Elmer) and a platereader (Synergy BioTek H1M), with fluorescence excitation and emission set to 485 nm and 515 nm, respectively. Background fluorescence was estimated using the fluorescence of a reaction containing no plasmid DNA. Fluorescence values units were converted into nM of GFP with the help of a calibration performed at 29 °C. A representative temporal response is shown in Supplementary Information G.

We used a +C construct as a positive control for the functioning of the breadboard reactions (*18*, *27*). These measurements are reported in Fig. 4B as a means to estimate the temperature dependence of a different construct to compare with that of the thermometers. The control (+C) has deGFP protein just like the thermometers in Fig. 4B. Further, the promoters (including UTR) have different sources, although the sequence of the RBS and between RBS and start codon is largely similar. The promoter of +C is the lambda re-

pressor Cro promoter (OR2-OR1-P_r) with UTR from the bacteriophage T7 gene 10 leader sequence (*27*). The promoter of the thermometers is based on a ribosomal RNA operon promoter P_{rrn} with a UTR consisting of an anti-SD sequence, a consensus SD sequence (5'-AAGGAG-3') followed by a spacer (8 nucleotides) derived from the bacteriophage T7 gene 10 leader sequence (*14*).

Acknowledgement

Supporting Information Available

The following files are available free of charge.

- A: Supplementary Table lists all RNA thermometer sequences.

- B: Supplementary Figure showing NUPACK analysis of +C sequence.

- C: Supplementary Figure showing the activity of RNA thermometer library in cell spots.

- D: Supplementary Figure showing correlation of sensitivities.

- E: Supplementary Figure showing detailed analysis of few individual thermometers.

- F: Supplementary Figure showing quantitation of activity in cell spots.

- G: Supplementary Figure showing temporal response of representative trace.

This material is available free of charge via the Internet at `http://pubs.acs.org/`.

References

1. Shapiro, M., Priest, M., Siegel, P., and Bezanilla, F. (2013) Thermal Mechanisms of Millimeter Wave Stimulation of Excitable Cells. Biophys J 104, 2622–2628.

2. Piraner, D. I., Abedi, M. H., Moser, B. A., Lee-Gosselin, A., and Shapiro, M. G. (2017) Tunable thermal bioswitches for in vivo control of microbial therapeutics. Nat Chem Biol 13, 75–80.

3. Hussain, F., Gupta, C., Hirning, A. J., Ott, W., Matthews, K. S., Josic, K., and Bennett, M. R. (2014) Engineered temperature compensation in a synthetic genetic clock. P Natl Acad Sci USA 111, 972–977.

4. Sen, S., Kim, J., and Murray, R. M. Designing robustness to temperature in a feedforward loop circuit. 2014 IEEE 53rd Annual Conference on Decision and Control (CDC). Los Angeles, USA, 2014; pp 4629–4634.

5. Pardee, K., Green, A. A., Ferrante, T., Cameron, D. E., DaleyKeyser, A., Yin, P., and Collins, J. J. (2014) Paper-based synthetic gene networks. Cell 159, 940–954.

6. Shin, J., and Noireaux, V. (2012) An E. coli cell-free expression toolbox: application to synthetic gene circuits and artificial cells. ACS Synth Biol 1, 29–41.

7. Takahashi, M. K., Hayes, C. A., Chappell, J., Sun, Z. Z., Murray, R. M., Noireaux, V., and Lucks, J. B. (2015) Characterizing and prototyping genetic networks with cell-free transcription-translation reactions. Methods 86, 60–72.

8. Niederholtmeyer, H., Sun, Z. Z., Hori, Y., Yeung, E., Verpoorte, A., Murray, R. M., and Maerkl, S. J. (2015) Rapid cell-free forward engineering of novel genetic ring oscillators. Elife 4, e09771.

9. Kortmann, J., and Narberhaus, F. (2012) Bacterial RNA thermometers: molecular zippers and switches. Nat Rev Microbiol 10, 255–265.

10. Morita, M. T., Tanaka, Y., Kodama, T. S., Kyogoku, Y., Yanagi, H., and Yura, T. (1999) Translational induction of heat shock transcription factor sigma32: evidence for a built-in RNA thermosensor. Genes Dev 13, 655–665.

11. Waldminghaus, T., Heidrich, N., Brantl, S., and Narberhaus, F. (2007) FourU: a novel type of RNA thermometer in Salmonella. Mol Microbiol 65, 413–424.

12. Kortmann, J., Sczodrok, S., Rinnenthal, J., Schwalbe, H., and Narberhaus, F. (2011) Translation on demand by a simple RNA-based thermosensor. Nucleic Acids Res 39, 2855–2868.

13. Altuvia, S., Kornitzer, D., Teff, D., and Oppenheim, A. B. (1989) Alternative mRNA structures of the cIII gene of bacteriophage lambda determine the rate of its translation initiation. J Mol Biol 210, 265–280.

14. Neupert, J., Karcher, D., and Bock, R. (2008) Design of simple synthetic RNA thermometers for temperature-controlled gene expression in *Escherichia coli*. Nucleic Acids Res 36, e124.

15. Neupert, J., and Bock, R. (2009) Designing and using synthetic RNA thermometers for temperature-controlled gene expression in bacteria. Nat Protoc 4, 1262–1273.

16. Jia, H., Sun, X., Sun, H., Li, C., Wang, Y., Feng, X., and Li, C. (2016) Intelligent Microbial Heat-Regulating Engine (IMHeRE) for Improved Thermo-Robustness and Efficiency of Bioconversion. ACS Synthetic Biology 5, 312–320.

17. Hoynes-O'Connor, A., Hinman, K., Kirchner, L., and Moon, T. S. (2015) *De novo* design of heat-repressible RNA thermosensors in *E. coli*. Nucleic Acids Res 43, 6166–6179.

18. Sun, Z. Z., Hayes, C. A., Shin, J., Caschera, F., Murray, R. M., and Noireaux, V. (2013) Protocols for implementing an Escherichia coli based TX-TL cell-free expression system for synthetic biology. J Vis Exp e50762.

19. Zadeh, J. N., Steenberg, C. D., Bois, J. S., Wolfe, B. R., Pierce, M. B., Khan, A. R., Dirks, R. M., and Pierce, N. A. (2011) NUPACK: Analysis and design of nucleic acid systems. J Comput Chem 32, 170–173.

20. Wang, Y.-H., Wei, K. Y., and Smolke, C. D. (2013) Synthetic Biology: Advancing the Design of Diverse Genetic Systems. Annu Rev Chem Biomol Eng 4, 69–102.

21. Chappell, J., Watters, K. E., Takahashi, M. K., and Lucks, J. B. (2015) A renaissance in RNA synthetic biology: new mechanisms, applications and tools for the future. Curr Opin Chem Biol 28, 47–56.

22. Bradley, R. W., Buck, M., and Wang, B. (2015) Tools and Principles for Microbial Gene Circuit Engineering. J Mol Biol 428, 862–88.

23. Sim, A. Y., Minary, P., and Levitt, M. (2012) Modeling nucleic acids. Curr Opin Struc Biol 22, 273–278.

24. Andersen, E. S. (2010) Prediction and design of DNA and RNA structures. New Biotechnol 27, 184–193.

25. Lucks, J. B., Qi, L., Mutalik, V. K., Wang, D., and Arkin, A. P. (2011) Versatile RNA-sensing transcriptional regulators for engineering genetic networks. P Natl Acad Sci USA 108, 8617–8622.

26. Narberhaus, F., Waldminghaus, T., and Chowdhury, S. (2006) RNA thermometers. FEMS Microbiol Rev 30, 3–16.

27. Shin, J., and Noireaux, V. (2010) Efficient cell-free expression with the endogenous E. Coli RNA polymerase and sigma factor 70. J Biol Eng 4, 8.

Graphical TOC Entry
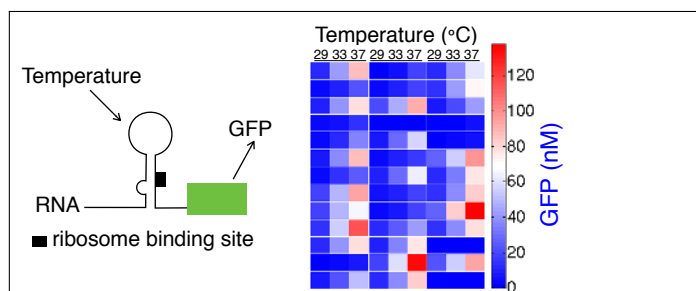
For Table of Contents Use Only.
Manuscript Title: Design of a Toolbox of RNA Thermometers
Authors: S Sen, D Apurva, R Satija, D Siegal, R M Murray